Proteomic And Metabolomic Analyses Reveal The Full Spectrum of Inflammatory and Lipid Metabolic Abnormalities In Dyslipidemia

Hui DU
Jiangxi University of Traditional Chinese Medicine
Yifei RAO
Jiangxi University of Traditional Chinese Medicine
Ronghua LIU
Jiangxi University of Traditional Chinese Medicine
Kesui DENG
The Affiliated Hospital of Jiangxi University of Traditional Chinese Medicine
Yongmei GUAN
Jiangxi University of Traditional Chinese Medicine
Dewei LUO
Jiangxi University of Traditional Chinese Medicine
Qiping MAO
Jiangxi University of Traditional Chinese Medicine
Jianwei YU
The Affiliated Hospital of Jiangxi University of Traditional Chinese Medicine
Tao BO
Thermo Fisher Scientific-CN
Ziquan FAN
Thermo Fisher Scientific-CN
hui ouyang (huiouyang@163.com)
Jiangxi University of Traditional Chinese Medicine https://orcid.org/0000-0002-4584-3357
Yulin FENG
State Key Laboratory Innovative Drug and Efficient Energy-Saving Pharmaceutical Equipment
Weifeng ZHU
Key Laboratory of Ministry of Education of Jiangxi University of Traditional Chinese Medicine

Research

Keywords: Dyslipidemia, Metabolomics, Proteomics, Biomarkers, Metabolic pathways

Posted Date: December 29th, 2020

DOI: https://doi.org/10.21203/rs.3.rs-135087/v1

Abstract

Background: Dyslipidemia is a common, chronic metabolic disease associated with cardiovascular complications. Due to the multiplicity of etiological factors, the pathogenesis of dyslipidemia is still unclear.

Methods: In this study, we combined proteomics and metabolomics methods to analyze the plasma of patients with dyslipidemia and healthy subjects. ITRAQ markers, combined with LC-MS/MS proteomics technology and the UHPLC/ Orbitfast-X Tribrid system, were used to establish the metabolite profile in clinical dyslipidemia.

Results: A total of 137 differentially expressed proteins were identified, mainly related to biological processes such as protein activation cascades, adaptive immune responses, complement activation, acute inflammatory responses and regulation of acute inflammatory responses. These proteins are involved in the regulation of important metabolic pathways, such as immunity and inflammation, coagulation and hemostasis, lipid metabolism, and oxidation and antioxidant defenses. Analysis of clinical metabolites showed there were 69 different metabolites in plasma, mainly related to glycerolipid, sphingolipid, porphyrin, alpha-linolenic acid, linoleic acid and arachidonic acid metabolism, suggesting that regulation of inflammation and lipid metabolism may be disturbed in patients with dyslipidemia. Among these, significant changes were observed in indole-3-propionic acid (IPA), which is considered a potential biomarker of dyslipidemia.

Conclusions: Combined analysis of proteins and metabolites showed that arachidonic acid, linoleic acid and lipid metabolic pathways were closely related to dyslipidemia. IPA may be a potential biomarker.The information provided in this study may provide new insights into the pathogenesis of dyslipidemia and related diseases, as well as potential intervention targets.

1. Introduction

Dyslipidemia is a common, chronic metabolic disease associated with cardiovascular complications [1]. It may occur in young adults (aged 21 to 39 years) and is an important risk factor for cardiovascular diseases [2]. Based on data collected between 2009 and 2012, > 100 million US adults ≥ 20 years of age have total cholesterol levels ≥ 200 mg/dL, and almost 31 million have levels ≥ 240 mg/dL. Between 2003 and 2012, the percentage of adults aged ≥ 40 years who had used a cholesterol-lowering medication in the past 30 days increased from 20–28% [3]. Dyslipidemia is characterized by abnormalities in lipid and lipoprotein metabolism, and most dyslipidemias are hyperlipidemias [4]. In preschool children, dyslipidemia is associated with a family history of disease [5]. There is significant heterogeneity in the prevalence of dyslipidemia and in the response to lipid-lowering drugs among different races or ethnicities [6]. In recent years, research on this condition has intensified. Dyslipidemia is a pathological condition that damages the endothelium, leading to cell proliferation, vascular remodeling, cell apoptosis and increased cell permeability, resulting in atherosclerotic lesions [7]. Unfortunately, the etiology of dyslipidemia is complex, so its pathogenesis is still unclear. Current clinical biomarkers, such as triglycerides, total cholesterol, LDL cholesterol, and HDL cholesterol, lack the necessary specificity and sensitivity and only increase significantly

after severe dyslipidemia [8]. Therefore, more sensitive and specific biomarkers are needed to improve early clinical diagnosis and treatment of the disease.

Modern technologies, such as proteomics and metabolomics, allow the specific detection and monitoring of metabolites associated with early changes in signal transduction and biochemical pathways. Thus, they can detect disease processes and drug effects before histopathological and pathophysiological changes occur [9]. The systematic analysis of large numbers of proteins expressed in a cell is an explicit goal of proteomics [10]. The protein domain is likely the most ubiquitously affected by diseases, and also during therapeutic response and recovery, so proteomics holds special promise for biomarker discovery [11]. Metabolomics is the untargeted analysis of the metabolome, which is comprised of low molecular weight molecules detected in a biological sample [12]. The metabolome holds a wealth of information that is thought to be most predictive of phenotype. Metabolites are the result of a combination of biological and environmental factors and thus offer great potential to analyze the association between genotypes and phenotypes [13]. The direct use of untargeted metabolomics to test individual patient samples and to perform interpretive comparisons with a controlled reference population is an emerging application known as "clinical metabonomics testing". Proteomics and metabolomics have been widely used to identify new sensitive and specific biomarkers [14]. However, it is difficult to elucidate all aspects of the etiological mechanisms of hyperlipidemia or the mechanisms of action of lipid-lowering drugs based on the study of single patients, so multi-group studies are needed. In this study, we combined proteomics and metabolomics techniques to conduct a systematic analysis of the plasma of patients with dyslipidemia. New biomarkers and metabolic pathways were identified, which may shed light on the underlying etiology and may serve to identify new therapeutic targets.

2. Materials And Methods

2.1. Ethical statement and clinical trial

This clinical study was conducted at the National Pharmaceutical Engineering Center For Solid Preparation in Chinese Herbal Medicine (NPEC). It was conducted from July until the end of September 2018, following the guidelines of the Ethics Committee of the Affiliated Hospital of Jiangxi University of Traditional Chinese Medicine(JXFYLL2017103013). All the volunteers were informed of the procedures and signed an informed consent form. Based on inclusion and exclusion criteria, 30 normal subjects and 30 dyslipidemia patients were selected. The diagnostic criteria for dyslipidemia were based on the 2016 Chinese Guideline for the Management of Dyslipidemia in Adults, formulated by a joint committee, and containing guidelines for the management of dyslipidemia in adults. These diagnostic criteria included hypercholesterolemia, hypertriglyceridemia, mixed hyperlipidemia or low HDL-C levels. Other inclusion criteria included ages between 18 and 70, eating a normal diet, and not taking medications or having taken medications one week prior to the study. Parameters were: serum total cholesterol (TC) ≥ 5.72 mmol /L, or triglycerides (TG) ≥ 2.26 mmol /L, or high-density lipoprotein (HDL-C) ≤ 1.04 mmol /L, or low-density lipoprotein (LDL-C) ≥ 3.64 mmol /L, within 2 weeks of the study. Exclusion criteria included persons younger than 18 or older than 70, incomplete clinical data, patients with mental diseases, cognitive impairment, impaired consciousness, speech and communication impediments, complicated tumors; severe liver or kidney diseases, cardiovascular diseases, pregnant or lactating women; severe acute somatic diseases or impaired organ

function. Fasting plasma samples were collected in the morning and stored at -80℃ for later use. The ages of the patients meeting the study requirements were analyzed for differences. The results are shown in Table 1. There was no significant difference between the normal and the dyslipidemia groups in terms of age.

Table 1
Study subject ages (n = 30, $\bar{\chi}$ ± s)

	age
normal group	29.07 ± 3.523
dyslipidemia group	28.14 ± 4.495
P value	0.386

2.2. Proteomic analysis

2.2.1. Protein extraction

A ProteoMiner protein enrichment kit (Bio-RAD Laboratories, California, USA) was used to selectively remove highly enriched proteins from plasma samples. Briefly, plasma samples were vortexed at a 10:1 ratio with lysis buffer (4% SDS, 1 mM DTT, 150 mM Tris-HCl, pH 8.0), heated in boiling water for 5 min, sonicated (80 W, 10 s ultrasound, intermittent 15 s, 10 times in total), heated once more in a boiling water bath for 5 min, and centrifuged at 16,000 g for 10 min at 4 ℃. Bicinchoninic acid (BCA) protein assay reagent (Solarbio, Beijing, China) was used to determine the protein concentration in the supernatant.

2.2.2. Filter-aided sample preparation (FASP) procedure and iTRAQ labeling

After adding DTT to 200 μg of protein sample (100 mM final concentration), samples were heated in boiling water for 5 min, and cooled to room temperature. UA buffer (8M urea, 150 mM Tris-HCl, pH 8.0) was added, samples were mixed, transferred to an ultrafiltration tube (10 Kd) and centrifuged (14,000 g, 4℃, 15 min) to separate the filtrate. Next, 50 mM iodoacetamide (IAA) (100μL) was added, samples were gently rocked (600 rpm, 1 min), and the reaction was allowed to proceed for 30 min in the dark, followed by centrifugation (14,000 g, 4℃, 10 min). Samples were washed twice with 100μL of UA buffer, centrifuged (14,000 g, 4℃, 10 min each time) and rinsed twice with 100μL of solution buffer. Next, DS buffer was added (40μL, with 2 μg trypsin), samples were gently mixed (600 rpm, 1 min), and digested overnight at 37℃. The collection tube was replaced with a new one, samples were centrifuged (14,000 g, 4℃, 10 min), and the resulting peptides were collected in the filtrate.

The resulting peptide mixture was labeled with the 8-plex iTRAQ kit (AB SCIEX, USA). The iTRAQ labeling method is described in the AB SCIEX iTRAQ labeling kit instructions. Briefly, the iTRAQ reagent was dissolved in 70μL of ethanol and added to 100 μg of the peptide mixture. Tubes were labeled as normal-113; normal − 114; normal − 115; normal − 116; disease − 117; disease − 118; disease − 119; and disease − 121, and vacuum dried.

2.2.3. Strong cation exchange (SCX) chromatographic separation of peptides

The iTRAQ-labeled peptides were fractionated by using an AKTA Purifier 100 system. The dried peptide mixture was acidified, dissolved in 2 mL of buffer A, and loaded onto the PolySULFOETHYL chromatography column (4.6 × 100 mm, 5 μm, 200 Å). The elution velocity was 1 mL/min, and the elution solvents were buffer A (10 mM KH2PO4 in 25% acetonitrile [ACN], pH 3.0) and buffer B (500 mM KCl, 10 mM KH2PO4 in 25% ACN, pH 3.0). The chromatographic column was balanced with buffer A, and the gradient elution procedure was as follows: 0–25 min, 0–10% B; 25–32 min, 10–20% B; 32–42 min, 20–45% B; 42–47 min, 45–100% B; and 47–60 min, 100% B. The elution process was monitored at 214 nm. The eluted fractions ware collected every 1 minute, and the freeze-dried fractions were desalinated with a C18 Cartridge. Peptides were quantitated after dissolving them in 40μL of solution buffer.

2.2.4. Liquid chromatography–tandem mass spectrometry (LC-MS/MS) analysis

The chromatographic column used was a Thermo Scientific EASY C18 column (75 m × 10 cm, 3 μm). Mobile phase A was aqueous 0.1% formic acid, and mobile phase B was 0.1% formic acid in aqueous solution: ACN 16/84 V/V. The elution velocity was 250 nL/min, and the gradient elution procedure was as follows: 0–50 min, 0–35% B; 50–58 min, 35–100% B; and 58–60 min, 100% B. MS data were collected for 60 min using a Q-Exactive mass spectrometer in positive ion detection mode (mass range 300–1800 m/z). The positive ion mode conditions were as follows: MS1 resolution (70,000); automatic gain control target (3e6); dynamic exclusion (40.0 s); maximum IT (10 ms); MS2 Activation Type (HCD); MS2 resolution (17,500); isolation window (2 m/z); normalized collision energy (30 eV); underfill ratio (0.1%).

2.2.5. Protein identification and quantitative analysis

Proteome Discoverer 1.4 software was used to identify and quantitatively analyze proteins based on the MS raw data and using Uniprot *Homo sapiens* sequences as reference (172,225 sequences, downloaded 2019/6/25). The peptide mass error and fragment mass error were set at ± 20 PPM and 0.1 Da, respectively. Protein quantification was performed based on the ratio calculated from the median of the unique peptide segments, and all peptide ratios were normalized to the median protein ratio to correct for experimental errors.

2.2.6. Bioinformatics analysis

Differentially expressed proteins were analyzed with GO (Functional annotation of Gene Ontology) based on known proteins annotated in the database, using Fisher's exact test to evaluate the significance level of different protein enrichments. The GO annotation steps for different proteins using Omicsbean software (http://www.omicsbean.cn/) were as follows: Sequence alignment (Blast), GO item extraction (Mapping), GO annotations and InterProScan supplemental annotations.

Proteins perform biological functions in organisms by coordinating their actions with other proteins. Since a single protein may be involved in different metabolic pathways, analysis of these related pathways is a

necessary step for a comprehensive understanding of their biological activities and association with disease. Kyoto Encyclopedia of Genes and Genomes (KEGG) enrichment analysis was used for this purpose. The total protein content was defined as the background, and Fisher's test was used to analyze the significance level of protein enrichment in each pathway. Thus, metabolic and signal transduction pathways that were significantly affected could be identified. Omicsbean software was used to annotate the KEGG pathway corresponding to the different proteins, and R version 3.5.1 software was used to generate the KEGG enrichment analysis bubble diagram.

Direct and indirect interaction relationships between different proteins were analyzed using the STRING (http://string-db.org/) database, and interaction networks were generated.

2.3. Metabolomics analysis

Working solution: 10.60 mg of 2-chloro-l-phenylalanine was carefully weighed and dissolved in 100 ml of methanol using a volumetric flask. This stock was diluted 10 times to prepare the working solution, with a concentration of 5.3 μg/mL. QC samples: 10μL from each plasma sample was vortexed and used as quality control samples. Plasma samples (50μL) were diluted with 200μL of working solution, vortexed for 30 s, and centrifuged (13,000 rpm, 4℃,10 min). The supernatant was transferred to an auto sampler vial for metabolomic analysis. To avoid the effects of fluctuations in the instrument detection signal, samples were analyzed continuously in random order. The quality control (QC) samples were processed in the same way as the plasma samples and were inserted into the sample queue to monitor the system's stability and to ensure the reliability of the experimental data. Metabolomic analysis was performed with a Orbitrap ID-X Tribrid mass spectrometer (Thermo Fisher), coupled to a Thermo Dionex Ultimate 3000 liquid chromatography system (Thermo Fisher), and equipped with an electrospray ionization (ESI) source. The chromatographic separations were performed using a Hypersil Gold C18 column (2.1 × 100 mm,1.9 μm). The column temperature was set to 45 ℃, the flow rate was 0.3 mL/min and the injection volume was 2 μ L. After optimization of the mobile phase, the positive and negative ion modes had different settings. The mobile phase in positive ion mode was A (0.1% formic acid in water) and B (0.1% formic acid + methanol). Gradient elution was optimized as follows: 0–8 min, 0%-50% B; 8–9 min, 50%-98% B; 9–13 min, 98% B; 13-13.1 min, 98%-0% B; 13.1–15 min, 0% B. The mobile phase in the negative ion mode was A (0.05% acetic acid in water) and B (methanol). Gradient elution was optimized as follows: 0–11 min, 2%-98% B; 11–13 min, 98% B; 13-13.1 min, 98%-2% B; 13.1–15 min, 2% B. MS data in the 70–1050 m/z range were intelligently collected using Q-Exactive Mass Spectrometer AcquireX. The conditions in negative ion mode (and positive ion mode) for ESI were as follows: spray voltage − 3200 V (3500 V); vaporizer temp 350℃; sheath gas 40 arb; aux gas 10 arb; capillary temp 320 ℃; MS1 resolution 120,000 FWHM; MS/MS resolution 30,000 FWHM.

2.3.1. Data processing

Raw data were imported to the Compound Discoverer software for analysis, including peak extraction, background subtraction, metabolite identification, multidimensional statistical analysis, and metabolic pathway analysis. First, the fractional composition and compound name were automatically matched with the best results in the Compound Discoverer software, based on the mass accuracy of the first and second

mass spectrometry results, isotope abundance ratio and mass spectrometry information in the database. Subsequently, the spectrogram was compared with the fragmentation patterns, including secondary or multiple levels of fragment ion information and related mass spectrometry data based on mzCloud, mzVault, and Chemspider databases. ChemSpider automatically runs mzLogic to establish a connection between mzCloud second-level fragment ion search and ChemSpider first-level structure for more reliable identification. The fragmentation Library™ database, with fragmentation tools and spectrographic auto annotation, allows the decomposition of different fragmentation ions and their corresponding structures to analyze the structure of compounds. Finally, MzLogic algorithm was used to analyze the correlation of identification results, integrate the identification results from different databases, and reorder and confirm the candidate metabolites, to increase the credibility of the identification results. We used Metabo Analyst 3.0 (http://www.metaboanalyst.ca) and KEGG online tools to analyze the different metabolites, the metabolic pathways involved, and for visualization.

3. Results

3.1. Protein characterization

This study successfully determined the plasma protein maps of patients with dyslipidemia and normal controls. A total of 218,812 plasma protein maps were obtained, 25,296 of which were matched with peptide segments. The total number of peptides was 4,170, and 601 proteins were identified. Detailed information on mass spectrometry collection and identification is shown in Table 2.

Table 2
Protein identification information

Database	Number of spectra	Number of peptide spectra	Number of peptides	Number of protein
Homo sapiens	218812	25296	4107	601

3.2. Identification of differentially expressed proteins

The identification of differentially expressed proteins was based on the fold change(FC > 1.2 or FC < 0.83, P value obtained by T test < 0.05)in expression between the normal group and the dyslipidemia group. The statistical results are shown in Table 3. A total of 137 differentially expressed proteins were identified between the normal group and the dyslipidemia group. Of these, 60 proteins were upregulated and 77 proteins were downregulated. The Volcano Plot in Fig. 1 summarizes these results. The x-coordinate represents the fold change difference (transformed with base 2 log), and the y-coordinate represents the p-value significance of the difference (transformed with base 10 log).

Table 3
Differentially expressed proteins between the normal group and the dyslipidemia group

Group name	Number of protein	Up-regulated protein	Down-regulated protein
normal group VS Dyslipidemia group	137	60	77

3.3. Cluster analysis of differentially expressed proteins

A hierarchical cluster algorithm was used to analyze the differentially expressed proteins and a heat map was drawn, as shown in Fig. 2. The y-coordinate represents significantly differentially expressed proteins, and the x-coordinate shows sample information. Differentially expressed proteins in the heat map are shown in different colors based on the amounts expressed in different samples (transformed with base 2 log). We observed that the protein expression profiles clearly fell into two categories, indicating that patients with dyslipidemia and normal subjects have significantly different plasma protein expression patterns.

3.4. Bioinformatics analysis

Fisher's test was used to analyze the GO function of proteins which were differentially expressed between the normal group and the dyslipidemia group, and the results are shown in Fig. 3A. The x-coordinate in this figure indicates the enriched GO functional classification, which is divided into three categories: Biological Process (BP), Cellular Component (CC) and Molecular Function (MF). The figure shows the top 10 enriched items in the BP, CC, and MF categories. The items in each category are ordered from left to right depending on their p value: the more to the left, the more significant their p value. The left ordinate represents the percentage of the corresponding proteins or genes with respect to the total number of proteins or genes, while the right ordinate represents the number of corresponding proteins or genes. Analysis showed significant changes in several Biological Processes (BP), including protein activation cascades, adaptive immune responses, complement activation, and regulation of acute responses, among others. There were also significant changes in Cellular Component (CC) items, including extracellular region, extracellular space, extracellular region part, blood microparticle and extracellular exosome, among others. Molecular Function (MF) showed significant changes in antigen binding, serine-type endopeptidase activity, endopeptidase inhibitor activity, endopeptidase regulator activity and peptidase inhibitor activity.

Fisher's test was used to conduct KEGG pathway enrichment analyses for differentially expressed proteins between the normal group and the dyslipidemia group, and the results are shown in Fig. 3B. The y ordinate represents the KEGG pathway that is enriched with the differentially expressed protein. The x ordinate represents the enrichment factor (Rich Factor ≤ 1) for the enriched KEGG pathway, and this represents the ratio of the number of differentially expressed proteins annotated in this KEGG pathway term to the total number of proteins annotated in this pathway term. The color gradient in the bubble represents the size of the P value, with the color fading from green to red. The closer the color is to red, the smaller the P value, and the higher the significance level of the corresponding KEGG pathway, indicating that this KEGG pathway has a higher correlation with dyslipidemia. The size of the bubble indicates the number of differentially expressed proteins enriched in the KEGG pathway. This analysis showed that pathways which were significantly altered included Complement and coagulation cascades, Staphylococcus aureus infection,

Osteoclast differentiation, Systemic Lupus erythematosus, Phagosome, Leishmaniasis, Natural killer cell mediated cytotoxicity and Tuberculosis, among others.

3.5. Protein-protein interaction network analysis (PPI)

A protein interaction network diagram was constructed for differentially expressed proteins between the normal and disease groups (Fig. 4). Nodes in Fig. 4 represent proteins, and lines represent interactions between proteins. Yellow nodes in the network represent differentially expressed proteins, whereas blue nodes represent other proteins included in the interaction network database which can interact directly with the differentially expressed proteins. This analysis revealed that dyslipidemia was highly associated with protein interactions related to complement, immunity, inflammation, coagulation, hemostasis, lipid metabolism, oxidation and anti- oxidation. The main proteins involved in immune and inflammatory responses were complement C4-B (C4B), immunoglobulin lambda-like polypeptide 5 (IGLL5), immunoglobulin iodine chain (VPREB1), low affinity immunoglobulin gamma Fc region receptor III-A (FCGR3A), and complement factor H-related protein 1 (CFHR1). The proteins involved in coagulation and hemostasis were: fibrinogen-like protein 1 (FGL1), coagulation factor XII (F12), histidine-rich glycoprotein (HRG), alpha-2-macroglobulin (A2M), and vitamin D-binding protein (GC). The proteins involved in lipid metabolism were: apolipoprotein C-IV (APOC4), apolipoprotein F (APOF), apolipoprotein D (APOD), apolipoprotein E (APOE), and apolipoprotein (a) (LPA). In terms of oxidation and anti-oxidation, the proteins were alpha-aminoadipic semialdehyde dehydrogenase (ALDH7AA), heat-stable enterotoxin receptor (GUCY2C) and adenylate cyclase type 6 (ADCY6).

3.6. Verification of metabolomics methodology

QC samples were interspersed in the procedure with the purpose of monitoring the operation status of the instrument and verifying the repeatability of the analytical method. Figure 5A shows an ion flow diagram of 7 QC samples, to monitor the reproducibility of the methodology. Figure 5B shows the RSD values at all ionic strengths in the QC group. RSD < 20% for more than 85% of compounds.

3.7. Metabolic profile analysis

Compound Discoverer software was used for multi-dimensional statistical analysis of metabolite data. A PCA score graph was constructed to observe the differences in the metabolic profiles between normal and dyslipidemia patients. The PCA score (Fig. 6) diagram clearly shows that QC samples cluster together, which proves that the instrument was in a stable state during the entire sample collection process. Figure 6 also shows that although there is partial overlap between the normal and dyslipidemia groups, there is an overall trend towards separation, which may be due to uncontrollable factors, which are normal phenomena in clinical sample analysis.

3.8. Screening and identification of potential biomarkers for dyslipidemia

Differences in plasma metabolites between the normal population and patients with dyslipidemia were identified by metabolic profile analysis. The Volcano Plot constructed with Compound Discoverer software, combined with S-plot analysis software, allows quick screening of differentially expressed metabolites.

Table 4 shows 69 differentially expressed metabolites identified based on $P \leq 0.05$ and $FC \geq 1.5$. Results mainly show a significant increase in ester levels and a decrease in the levels of some indoles. The heatmap in Fig. 7 shows changes in metabolites in each individual, reflecting the differing trends in metabolite expression between patients with dyslipidemia and the normal population. Red represents an increasing trend in metabolite levels, green represents a decreasing trend in metabolite levels, and the color brightness reflects the degree of change. Interestingly, the normal and disease groups were roughly divided into two. In addition, indole-3-propionic acid (IPA) levels were significantly reduced in the disease group while ester levels were generally upregulated in the disease group.

Table 4
Identification of potential biomarkers in human plasma samples, based on analysis of healthy subjects and dyslipidemia patients.

NO	Retention Time	Name	formula	Molecular Weight	Ion Mode	Levels
P1	6.56	Indole-3-propionic acid	C11H11NO2	189.0793	[M-H]-	↓
P2	3.97	Indole-3-acrylic acid	C11H9NO2	187.0631	[M + H]+	↓
P3	7.13	4-ethylphenylsulfonic acid	C8H10O4S	202.0302	[M-H]-	↓
P4	6.56	Indole-3-propionic acid	C11H11NO2	189.0793	[M + H]+	↓
P5	9.63	Bilirubin	C33H36N4O6	584.2631	[M + H]+	↓
P6	10.78	Deoxycholic acid	C24H40O4	392.2934	[M-H]-	↓
P7	12.52	DG (42:5)	C45H78O5	698.5881	[M + H]+	↓
P8	11.48	MG (24:5)	C27H44O4	432.3249	[M-H]-	↓
P9	12.53	DG (22:2_22:6)	C47H76O5	720.5699	[M + H]+	↓
P10	11.36	LPS (22:6)	C28H44NO9P	569.2745	[M-H]-	↑
P11	11.53	LPS (26:4)	C32H56NO9P	629.3710	[M-H]-	↑
P12	2.65	CAR (8:1(OH))	C15H27NO5	301.1894	[M-H]-	↑
P13	11.22	LPS (20:0)	C26H52NO9P	553.3395	[M-H]-	↑
P14	11.50	LPE (22:5)	C27H46NO7P	527.3025	[M-H]-	↑
P15	11.80	LPS (26:3)	C32H58NO9P	631.3867	[M-H]-	↑
P16	11.50	LPE (22:5)	C27H46NO7P	527.3025	[M + H]+	↑
P17	11.58	LPE (20:3)	C25H46NO7P	503.3024	[M-H]-	↑
P18	5.34	CAR (10:0(6Ke))	C17H31NO5	329.2199	[M + H]+	↑

NO	Retention Time	Name	formula	Molecular Weight	Ion Mode	Levels
P19	11.49	LPS (24:2)	C30H56NO9P	605.3709	[M-H]-	↑
P20	11.09	FA (20:3)	C20H32O3	320.2357	[M-H]-	↑
P21	11.36	LPS (26:5)	C32H54NO9P	627.3554	[M-H]-	↑
P22	11.33	LPE (22:6)	C27H44NO7P	525.2868	[M-H]-	↑
P23	11.25	16,17-epoxy-DHA	C22H30O3	342.2201	[M-H]-	↑
P24	11.75	1-Palmitoyl-2-sn-glycero-3-phosphatidylcholine	C32H58NO11P	663.3742	[M-H]-	↑
P25	11.89	LPS (24:1)	C30H58NO9 P	607.3867	[M-H]-	↑
P26	2.95	12-Aminododecanoic acid	C12H25NO2	215.1883	[M+H]+	↑
P27	11.39	PS (O-18:0/18:2)	C42H80NO9 P	773.5563	[M+H]+	↑
P28	10.23	LPA (14:0)	C17H35O7P	382.2119	[M+H]+	↑
P29	10.75	LPE (P-18:1)/LPE (O-18:2)	C23H46NO6 P	463.3058	[M+H]+	↑
P30	11.70	SM (d18:2/14:0)	C37H73N2O6P	672.5200	[M+H]+	↑
P31	11.53	LPS (26:4)	C32H56NO9P	629.3710	[M+H]+	↑
P32	12.25	SM (d17:1/18:3)	C40H75N2O6P	710.5333	[M+H]+	↑
P33	11.84	LPS(O-20:0)	C26H54NO8P	539.3601	[M-H]-	↑
P34	11.75	1-Palmitoyl-2-(5-keto-6-octendioyl)-sn-glycero-3-phosphatidylcholine	C32H58NO11P	663.3742	[M+H]+	↑
P35	12.19	LPE(P-18:0)/LPE(O-18:1)	C23H48NO6P	465.3226	[M-H]-	↑
P36	11.06	Arachidonic acid methyl ester	C21H34O2	318.2556	[M+H]+	↑
P37	12.38	N-Palmitoylsphingosine	C34H67NO3	537.5117	[M+H]+	↑

NO	Retention Time	Name	formula	Molecular Weight	Ion Mode	Levels
P38	10.40	16(R)-HETE	C20H32O3	342.2193	[M + H]+	↑
P39	10.75	CAR (18:1(11E))	C25H47NO4	425.3498	[M + H]+	↑
P40	10.72	LPC (22:4)	C30H54NO7P	571.3632	[M + H]+	↑
P41	10.75	LPE(P-18:1)/LPE(O-18:2)	C23H46NO6P	463.3058	[M + H]+	↑
P42	10.7	LPE (P-16:0)/LPE(O-16:1)	C21H44NO6P	437.2902	[M + H]+	↑
P43	11.38	LPS (24:3)	C30H54NO9P	603.3554	[M-H]-	↑
P44	13.71	SM (d18:0/22:3)	C45H85N2O6P	780.6112	[M + H]+	↑
P45	10.92	LPE(P-18:0)	C23H48NO6P	465.3215	[M + H]+	↑
P46	11.33	LPE (22:6)	C27H44NO7P	525.2868	[M-H]-	↑
P47	11.58	Glycerophospho-N-palmitoyl ethanolamine	C21H44NO7P	453.2865	[M-H]-	↑
P48	10.79	LPC (20:2)	C28H54NO7P	547.3634	[M + H]+	↑
P49	13.81	PC (16:0_22:4)	C46H84NO8P	809.5900	[M + H]+	↑
P50	11.36	LPS (26:5)	C32H54NO9P	627.3554	[M-H]-	↑
P51	11.22	LPS (20:0)	C26H52NO9P	553.3395	[M-H]-	↑
P52	11.29	LPS (22:1)	C28H54NO9P	579.3552	[M-H]-	↑
P53	13.47	PC (18:0_22:6)	C48H84NO8P	833.5906	[M + H]+	↑
P54	12.10	SM(d18:1/18:4)	C41H75N2O6P	722.5327	[M + H]+	↑
P55	6.70	9-Oxononanoicacid	C9H16O3	172.1101	[M-H]-	↑
P56	12.25	SM(d16:1/17:0)	C38H77N2O6P	688.5514	[M + H]+	↑

NO	Retention Time	Name	formula	Molecular Weight	Ion Mode	Levels
P57	13.02	DL-Dipalmitoylphosphatidylcholine	C40H80NO8P	733.5616	[M + H]+	↑
P58	13.71	SM(d16:1/22:0)	C43H87N2O6P	758.6295	[M + H]+	↑
P59	11.41	MG (26:4)	C29H50O4	462.3706	[M + H]+	↑
P60	12.03	SM(d16:0/16:1)	C37H75N2O6P	674.5357	[M + H]+	↑
P61	12.25	N-Palmitoyl taurine	C18H37NO4S	726.4982	[M + H]+	↑
P62	11.38	LPS (24:3)	C30H54NO9P	603.3554	[M-H]-	↑
P63	13.02	SM(d18:1/18:0)	C41H83N2O6P	730.5984	[M + H]+	↑
P64	11.75	LPS (22:0)	C28H56NO9P	581.3708	[M-H]-	↑
P65	10.65	LPC (20:3)	C28H52NO7P	545.3473	[M + H]+	↑
P66	10.91	Linoleic acid-biotin	C28H48N4O3S	1084.6735	[M + H]+	↑
P67	10.55	LPC (20:4)	C28H50NO7P	543.3320	[M + H]+	↑
P68	10.91	LPC (18:0)	C26H54NO7P	523.3633	[M + H]+	↑
P69	10.67	1-Palmitoylglycerophosphocholine	C24H50NO7P	495.3319	[M + H]+	↑

3.9. Analysis of metabolic pathways in dyslipidemia

Figure 8 shows the enrichment pathway results, based on MetaboAnalyst and KEGG common platforms for the analysis of enrichment of potential biomarkers and topological analysis. Differences between patients with dyslipidemia and the normal population reside mainly in glycerolipid, sphingolipid, porphyrin, alpha-linolenic acid, linoleic acid and arachidonic acid metabolism.

4. Discussion

4.1. Proteomic analysis

Differentially expressed proteins between clinical dyslipidemia and normal samples were studied using iTRAQ marker quantitative proteomics technology. A total of 137 differentially expressed proteins were

identified between the normal group and the dyslipidemia group. Of these, 60 proteins were upregulated and 77 were downregulated. Based on Functional Annotation of Gene Ontology (GO) analysis, it was found that most proteins in the Biological Process (BP) category were related to defense response processes, followed by adaptive immune responses. Cellular Component (CC) analysis showed that most proteins were located in the extracellular region (extracellular domain), indicating that the extracellular response to dyslipidemia was relatively active. Molecular Function (MF) analysis showed that the differentially expressed proteins were involved with antigen binding, and the immune response involves antigen-antibody binding.

Differentially expressed proteins were analyzed with the KEGG database to explore their potential biological functions. "Complement and coagulation cascade" was the most common pathway, followed by "Staphylococcus aureus infection" and "metabolic pathway". These annotated protein types are mainly related to extracellular matrix (ECM) -receptor interactions, phagocytes, PI3K-Akt signaling pathway, platelet activation, systemic lupus erythematosus, local adhesion and the Rap1 signaling pathway. The complement and coagulation cascades involve a series of synergistic calcium-dependent proenzyme-serine protease transformations that occur on the surface of activated cells and which trigger the release of vasoactive kinin. They are involved in many physiological and pathological processes, such as sodium and blood pressure regulation, and inflammatory related processes.

Analysis of protein-protein interactions showed that the differences in patients with dyslipidemia were mainly associated with immunity and inflammation, coagulation and hemostasis, lipid metabolism, oxidation and antioxidation. Studies have shown that dyslipidemia can trigger a variety of pathophysiological events, including inflammation, cell damage and, especially, oxidative stress [15]. Elevated levels of inflammatory factors in dyslipidemia can activate macrophages, neutrophils, endothelial cells and other related inflammatory cells, resulting in endothelial damage and increased permeability, leading to leukocyte adhesion and the release of a large number of cytokines [16]. Compared with the normal group, dyslipidemia patients had altered levels of apolipoproteins associated with lipid metabolism. By using virtual proteomics technology, Mosley JD [17] et al. found that apolipoprotein levels were linked to dyslipidemia. Apolipoprotein C-I is a plasma protein secreted by fat cells which is a predictive marker of cardiovascular disease [18]. Apolipoprotein A and Apolipoprotein E are involved in lipid metabolism, and can enhance the outflow of cholesterol from cells, preventing atherosclerosis in the arterial wall [19]. Apolipoprotein C-IV (APOC4), apolipoprotein F (APOF), apolipoprotein D (APOD), apolipoprotein E (APOE), and apolipoprotein a (LPA) were altered in patients with dyslipidemia, and studies have shown that apolipoprotein alterations interfere with the regulation of immunity and inflammation. Apolipoproteins can regulate inflammation and oxidative stress by inhibiting T cell proliferation and promoting the delivery of lipid antigens, regulating macrophage function [20].

4.2. Metabolomics analysis

Plasma metabolites which were differentially expressed between patients with dyslipidemia and healthy subjects were studied using metabonomics technology, and 69 potential biomarkers were identified. Enrichment and topological analyses of metabolic pathways revealed that glycerolipid, sphingolipid, porphyrin, alpha-linolenic acid, linoleic acid, and arachidonic acid metabolic pathways were closely related to dyslipidemia.

Clinical metabonomics showed that certain organic acids showed significant changes in the plasma of dyslipidemia patients, and that indole propionic acid was a characteristic biomarker. Compared with normal subjects, the indole-3-propionic acid (IPA) content in plasma was decreased in patients with dyslipidemia, in both the positive and negative ion modes. IPA is a tryptophan metabolite which can play an antioxidant role by scavenging hydroxyl free radicals in the body [21]. Studies have shown that IPA is an effective neuroprotective agent against a variety of oxidative toxins. It can reduce DNA damage in neurons and attenuate lipid peroxidation *in vivo* [22]. The latest study also found that IPA, a metabolite produced by the gut microbiota, protects β cell function and may serve as a potential biomarker for the development of type 2 diabetes mellitus (T2D) [23].

The blood lipid content in patients with dyslipidemia is ~ 1.2–2 times higher than that of normal subjects. These changes mainly involve increased levels of hemolytic phospholipids [LPC(22:4), LPC(20:2), LPC(20:2), LPC(20:4), LPC(18:0), etc.], arachidonic acid metabolites (arachidonic acid methyl ester, 16(R)-HETE, etc.) and other partially oxidized lipids. Studies suggest that lipid peroxides may be the cause of atherosclerosis [24]. In addition, based on studies of the IPA biomarker and its anti-lipid peroxidation effect, it is speculated that the increased plasma oxidized lipid content in patients with dyslipidemia may be caused by a reduction in IPA content. The specific mechanism of action needs to be studied further. In addition, plasma bilirubin and partial bile acids (bilirubin, deoxycholic acid, etc.) were also found to be reduced in patients with dyslipidemia. Bilirubin has certain antioxidant effects: it can effectively remove hydrogen peroxide groups, protect lipid films from oxidation by active groups, and inhibit the oxidation of linoleic acid and phospholipids. Lipopolysaccharide (LPS) is the main component of the outer membrane of Gram-negative bacteria [25]. Studies have shown that low levels of LPS can be detected in the blood of healthy subjects [26]. In this study we found that several LPS metabolites [LPS(22:6), LPS(26:4),LPS(20:0), LPS(26:3), etc.] were upregulated, and LPS can promote metabolic inflammation and insulin resistance[27].

Linoleic acid is an unsaturated fatty acid. Due to the antioxidant activity of its double bonds, it can regulate lipid metabolism in the body and help improve lipid levels [28]. Arachidonic acid can be produced from linoleic acid by a multistep reaction. Since it is the precursor of most leukotrienes and prostaglandins, arachidonic acid can increase plasma lipoxygenin A4 (LXA4) through a series of reactions to produce an anti-inflammatory effect. In this study, we found abnormal arachidonic acid metabolism in patients with dyslipidemia, which is consistent with a previous study reporting that hypercholesterolemia leads to changes in arachidonic acid metabolism [29]. Sphingolipids are a large class of lipids with structural and signaling functions. They are abundant in mammalian plasma, and up to 18% of plasma phospholipids exist in the form of sphingolipids [30]. Abnormal sphingolipid metabolism has been demonstrated in atherosclerosis [31].

4.3. Combined proteomics and metabolomics analysis

Combined analysis of proteins and metabolites showed that arachidonic acid, linoleic acid and lipid metabolic pathways were closely related to dyslipidemia.

Arachidonic acid and linoleic acid metabolism are classic inflammation-related pathways. Inflammation is closely related to dyslipidemia and can lead to changes in lipid metabolism. Chronic inflammation can lead

to diseases such as atherosclerosis and metabolic syndrome [32]. Atherosclerosis is increasingly recognized as an inflammatory disease and the interaction between lipid metabolism and inflammatory pathways has a direct impact on the development of atherosclerosis [33].

5. Conclusions

In summary, iTRAQ labeling combined with LC-MS/MS proteomics were used to identify plasma proteins which were differentially expressed between patients with dyslipidemia and normal subjects. A total of 137 differentially expressed proteins were identified, mainly located in the extracellular space, and related to biological processes such as protein activation cascades, adaptive immune responses, complement activation, acute inflammatory responses and regulation of acute inflammatory responses. They are involved in the regulation of important pathways such as immunity and inflammation, coagulation and hemostasis, lipid metabolism, oxidation and antioxidant defenses. Analysis of plasma with the UHPLC/OrbitrapID - X Tribrid system identified 69 potential biomarkers of dyslipidemia, mainly associated with glycerolipid, sphingolipid, porphyrin, alpha-linolenic acid, linoleic acid and arachidonic acid metabolism. Combined analysis of proteins and metabolites showed that arachidonic acid, linoleic acid and lipid metabolic pathways were closely related to dyslipidemia. In addition, we found that IPA may be a potential biomarker. However, the precise mechanisms of action need to be investigated further. The combined application of multiple techniques can improve our understanding of dyslipidemia, providing a theoretical framework for future studies on lipid lowering drugs.

Abbreviations

ITRAQ
Isobaric tags for relative and absolute quantification
IPA
Indole-3-propionic acid
LDL-C
Low-Density Lipoprotein cholesterol
HDL-C
High-Density Lipoprotein cholesterol
NPEC
The National Pharmaceutical Engineering Center For Solid Preparation in Chinese Herbal Medicine
TC
Total cholesterol
TG
Triglycerides
FASP
Filter-aided sample preparation
SCX
Strong cation exchange
LC-MS/MS

Liquid chromatography–tandem mass spectrometry
GO
Functional annotation of Gene Ontology
KEGG
Kyoto Encyclopedia of Genes and Genomes
QC
Quality control
FC
Fold change
PPI
Protein-protein interaction network analysis

Declarations

- Ethics approval and consent to participate

This study has been approved by the ethics committee of the Affiliated Hospital of Jiangxi University of Traditional Chinese Medicine, conducted from July until the end of September 2018.

Each patient submitted written informed consent to participate in the study.

- Consent for publication

Not applicable.

- Availability of data and materials

Not applicable.

- Competing interests

The authors declare no competing financial interests.

- Authors' contributions

H.O., Y.F. and W.Z. designed the research, H.D., Y.R., T.B. and Z.F. did the experiment, H.D., Y.R., R.L., K.D., Y.G., D.L., Q.M.,J.Y., H.O., Y.F. and W.Z. analyzed data, H.D. and Y.R. wrote the manuscript.

- Acknowledgements

This study was supported by the National Key R&D Program of China (2017YFC1702902 and 2019YFC1712300), Jiangxi university of traditional Chinese medicine 1050 youth talent project, "Double Hundred Plan" for high-level scientific and technological innovation talents in Nanchang (China).

References

1. Kopin L, Lowenstein C. Dyslipidemia Annals of Internal Medicine. 2007;35:529–33.
2. Chou R, Dana T, Blazina I, et al. Screening for Dyslipidemia in Younger Adults: A Systematic Review for the U.S. Preventive Services Task Force. Ann Intern Med. 2016;165:560.
3. Members WG, Mozaffarian D. Benjamin E J, et al. Executive Summary: Heart Disease and Stroke Statistics–2016 Update: A Report From the American Heart Association. Circulation. 2016;127:143–52.
4. Sukhorukov VN, Karagodin VP, Orekhov AN. Modern methods of diagnosis dyslipidemia. Patologicheskaia Fiziologiia I Eksperimentalnaia Terapiia. 2016;60:65.
5. Guerrero-Romero F, Martha R-M. Prevalence of dyslipidemia in non-obese prepubertal children and its association with family history of diabetes, high blood pressure, and obesity. Arch Med Res. 2006;37:1015–21.
6. Jia Pu. Robert, et al. Dyslipidemia in Special Ethnic Populations. Cardiol Clin. 2015;33:325–33.
7. Hurtubise J, Mclellan K, Durr K, et al. The Different Facets of Dyslipidemia and Hypertension in Atherosclerosis. Current Atherosclerosis Reports. 2016;18:82.
8. Chen H, Miao H, Feng YL, et al. Metabolomics in Dyslipidemia Advances in Clinical Chemistry. 2014;66:101–19.
9. Christians U, Schmitz V, Klawitter J, et al. Proteo-Metabolomic Strategies in the Future of Drug Development. Analytical Techniques for Clinical Chemistry. Wiley-Blackwell. 2012.
10. Aebersold R. Mann, et al. Mass spectrometry-based proteomics. Nature, 2003.
11. Rifai N. Gillette, et al. Protein biomarker discovery and validation: the long and uncertain path to clinical utility. Nature Biotechnology. 2006.
12. Kennedy AD, Wittmann BM, Evans AM, et al. Metabolomics in the clinic: A review of the shared and unique features of untargeted metabolomics for clinical research and clinical testing. J Mass Spectrom. 2018;53:ii–i.
13. Schrimpe-Rutledge AC, Codreanu SG, Sherrod SD, et al. Untargeted Metabolomics Strategies—Challenges and Emerging Directions. J Am Soc Mass Spectrom. 2016;27:1897–905.
14. Lo DJ, Kaplan B, Kirk AD.. Biomarkers for kidney transplant rejection. Nature Reviews Nephrology. 2014.
15. Anel Gómez-García, Gloria Martínez Torres, Ortega-Pierres LE,et al.Rosuvastatin and metformin decrease inflammation and oxidative stress in patients with hypertension and dyslipidemia. Revista Espanola De Cardiologia. 2007; 60:1242–1249.
16. Hurtubise J, Mclellan K, Durr K, et al. The Different Facets of Dyslipidemia and Hypertension in Atherosclerosis. Current Atherosclerosis Reports. 2016;18:82.
17. Mosley JD, Benson MD, Smith JG, et al. Probing the Virtual Proteome to Identify Novel Disease Biomarkers. Circulation. 2018;138:2469–81.
18. Li RX, Ding YB, Zhao SL, et al. Secretome-derived isotope tags (SDIT) reveal adipocyte-derived apolipoprotein C-I as a predictive marker for cardiovascular disease. J Proteome Res. 2012;11:2851.
19. Kaga E, Karademir B, Baykal AT, et al. Identification of differentially expressed proteins in atherosclerotic aorta and effect of vitamin E. J Proteom. 2013;92:260–73.

20. Zhang HL, Wu J, Zhu J. The Role of Apolipoprotein E in Guillain-Barré Syndrome and Experimental Autoimmune Neuritis. Journal of Biomedicine and Biotechnology. 2010; 2010:1–12.
21. William R, Wikoff AT, Anfora J, Liu, Peter G, Schultz SA, Lesley EC, Peters Steve A. Metabolomics analysis reveals large effects of gut microflora on mammalian blood metabolites. Proc Natl Acad Sci USA. 2009;106:3698–703.
22. Chyan Y-J, et al. Potent neuroprotective properties against the Alzheimer β-amyloid by an endogenous melatonin-related indole structure, indole-3-propionic acid. J Biol Chem. 1999;274:21937–42.
23. De Mello VD, Paananen J, Lindstr?M J, et al. Indolepropionic acid and novel lipid metabolites are associated with a lower risk of type 2 diabetes in the Finnish Diabetes Prevention Study. entific Reports. 2017;7:46337.
24. Stringer MD, Gorog PG, Freeman A, et al. Lipid peroxides and atherosclerosis. BMJ. 1989;298:281–4.
25. Rodney D, Berg. The indigenous gastrointestinal microflora. Trends Microbiol. 1996;4:0–435.
26. Goto T, Edén S, Nordenstam G, et al. Endotoxin levels in sera of elderly individuals. Clinical Diagnostic Laboratory Immunology. 1994;1:684–8.
27. Caesar R, F?K F, B?Ckhed F.. Effects of gut microbiota on obesity and atherosclerosis via modulation of inflammation and lipid metabolism. Journal of Internal Medicine. 2010; 268.
28. Hartigh LJD, Han CY, Wang S, et al. 10E,12Z-conjugated linoleic acid impairs adipocyte triglyceride storage by enhancing fatty acid oxidation, lipolysis, and mitochondrial reactive oxygen species. J Lipid Res. 2013;54:64–78.
29. Goodwill AG, Stapleton PA, James ME, et al. Increased Arachidonic Acid-Induced Thromboxane Generation Impairs Skeletal Muscle Arteriolar Dilation with Genetic Dyslipidemia. Microcirculation. 2010;15:621–31.
30. Nilsson A, Duan RD. Absorption and lipoprotein transport of sphingomyelin. J Lipid Res. 2006;47:154.
31. Jiang XC, Liu J.. Sphingolipid Metabolism and Atherosclerosis. Sphingolipids in Disease. Springer Vienna. 2013; 133.
32. Esteve E, Ricart W. José Manuel Fernández-Real. Dyslipidemia and inflammation: an evolutionary conserved mechanism. Clin Nutr. 2005;24:16–31.
33. Van Diepen JA, Berbée, Jimmy FP, Havekes LM, et al. Interactions between inflammation and lipid metabolism: Relevance for efficacy of anti-inflammatory drugs in the treatment of atherosclerosis. Atherosclerosis. 2013;228:306–15.

Figures

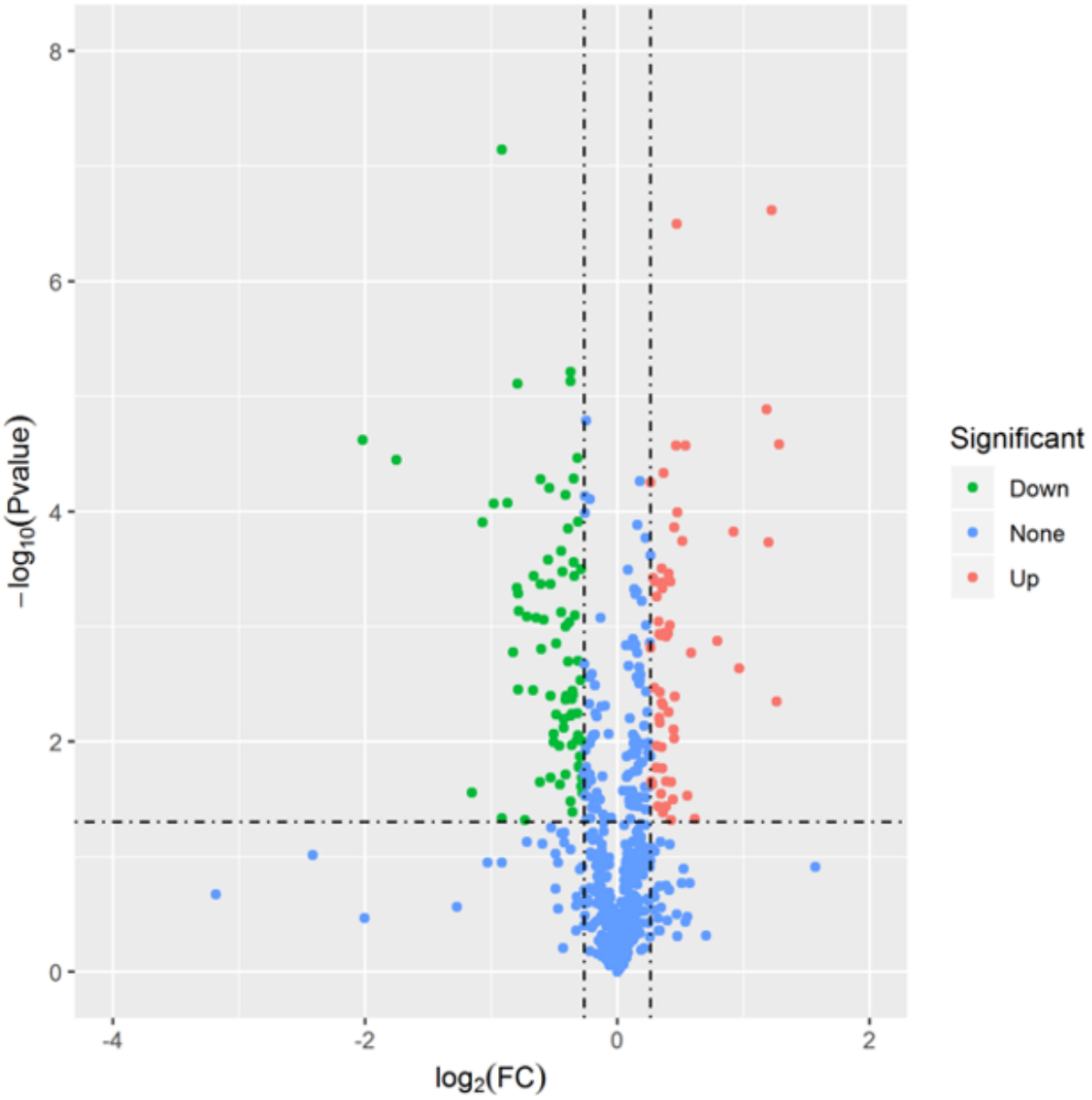

Figure 1

Volcano map of differentially expressed proteins in normal vs dyslipidemia groups (red dots are significantly upregulated proteins, green dots are significantly downregulated proteins, and blue dots are proteins showing no significant change)

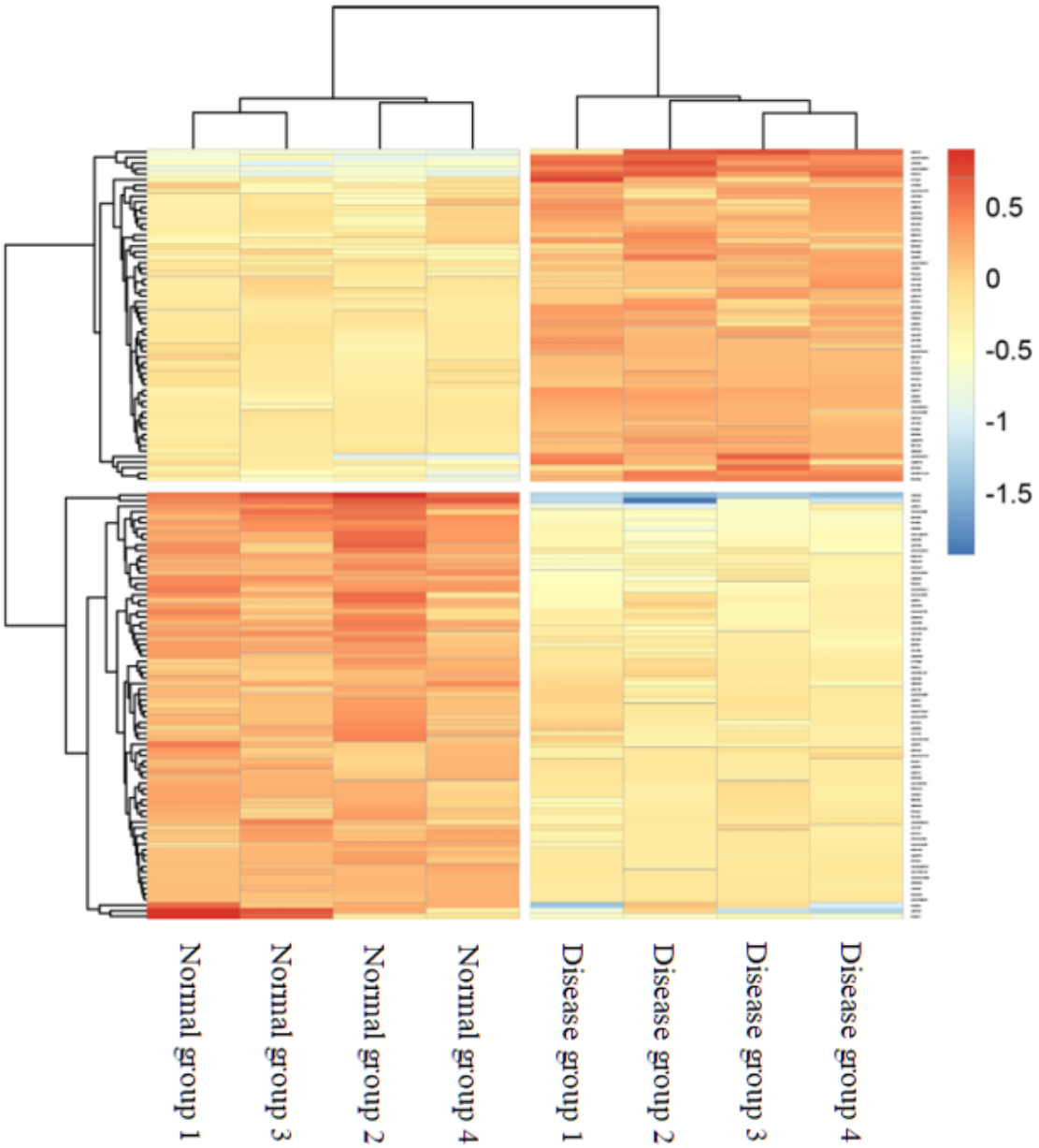

Figure 2

Cluster analysis of differentially expressed proteins in normal vs dyslipidemia groups (red represents relatively high protein content, and blue represents relatively low protein content)

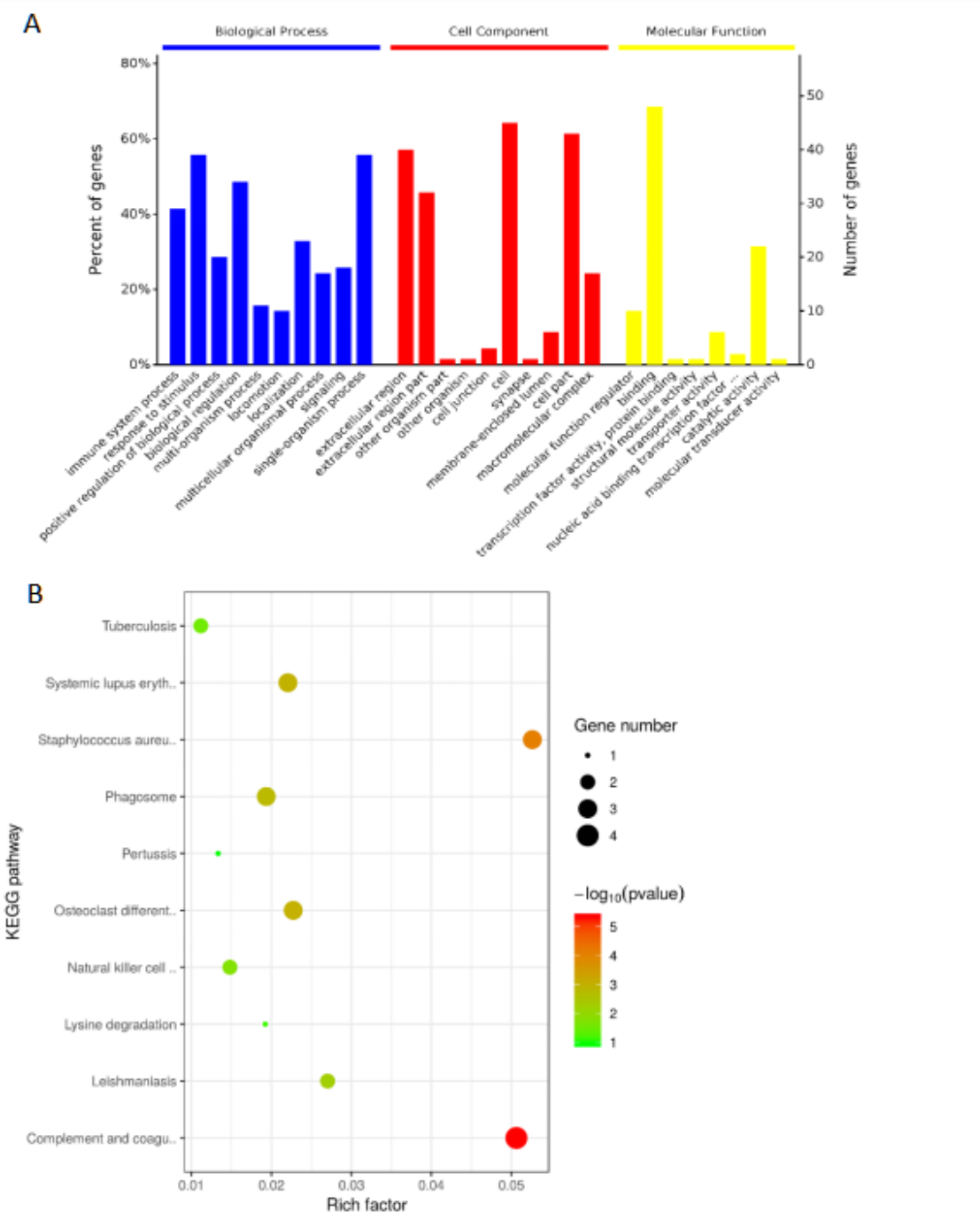

Figure 3

Bioinformatics analysis (A) GO function enrichment analysis (B) KEGG pathway enrichment analysis

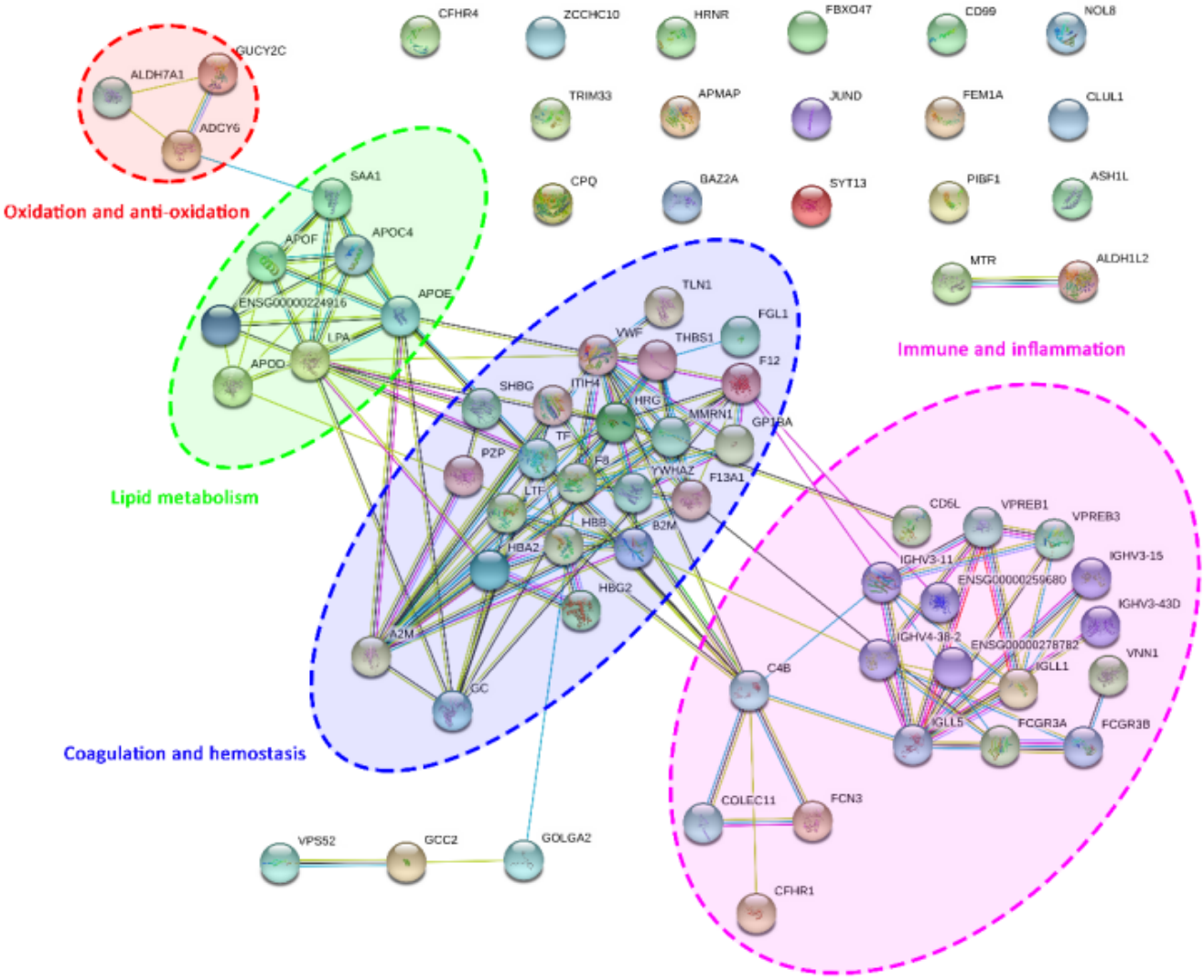

Figure 4

Interaction network for differentially expressed proteins between the normal and dyslipidemia groups

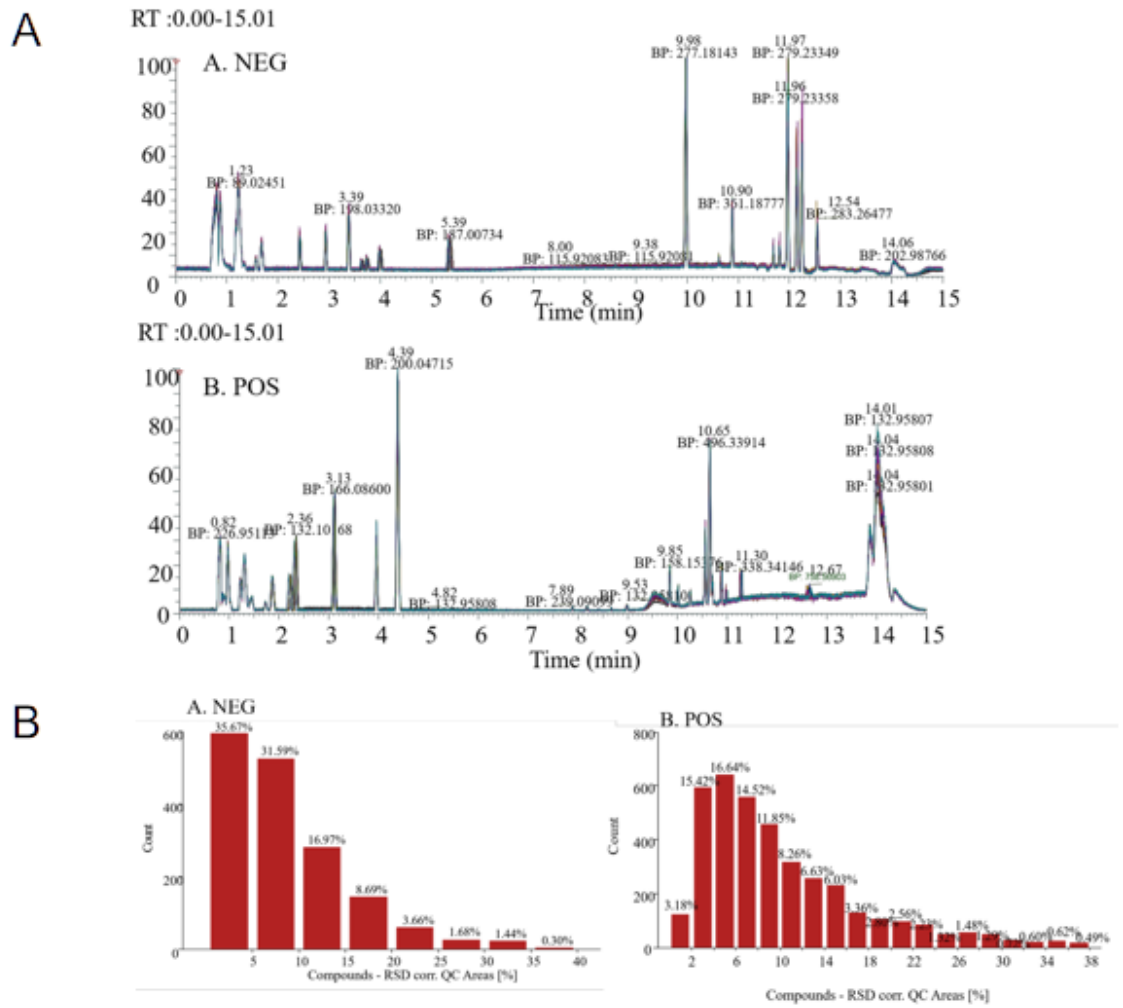

Figure 5

Verification of metabolomics methodology (A) BPI of QC sample (A. Negative ion mode; B. Positive ion mode) (B) RSD% in the QC group (n = 7, A. Negative ion mode; B. Positive ion mode)

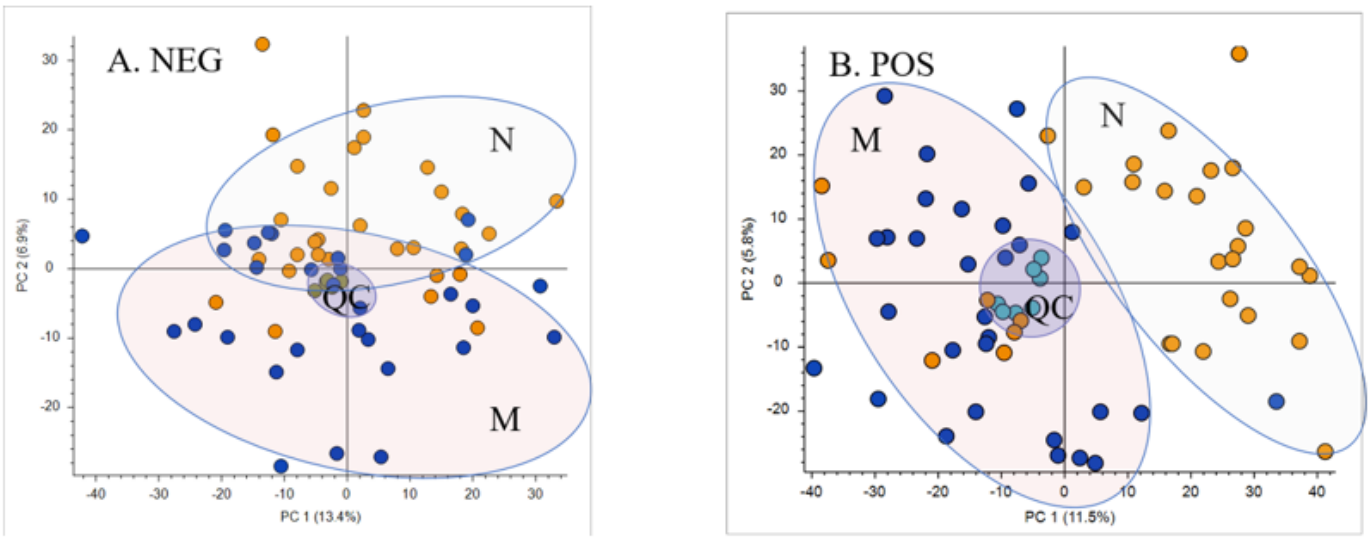

Figure 6

PCA score plots of normal and dyslipidemia model groups (A. Negative ion mode; B. Positive ion mode; N. Normal group, M. Model group, QC. QC group)

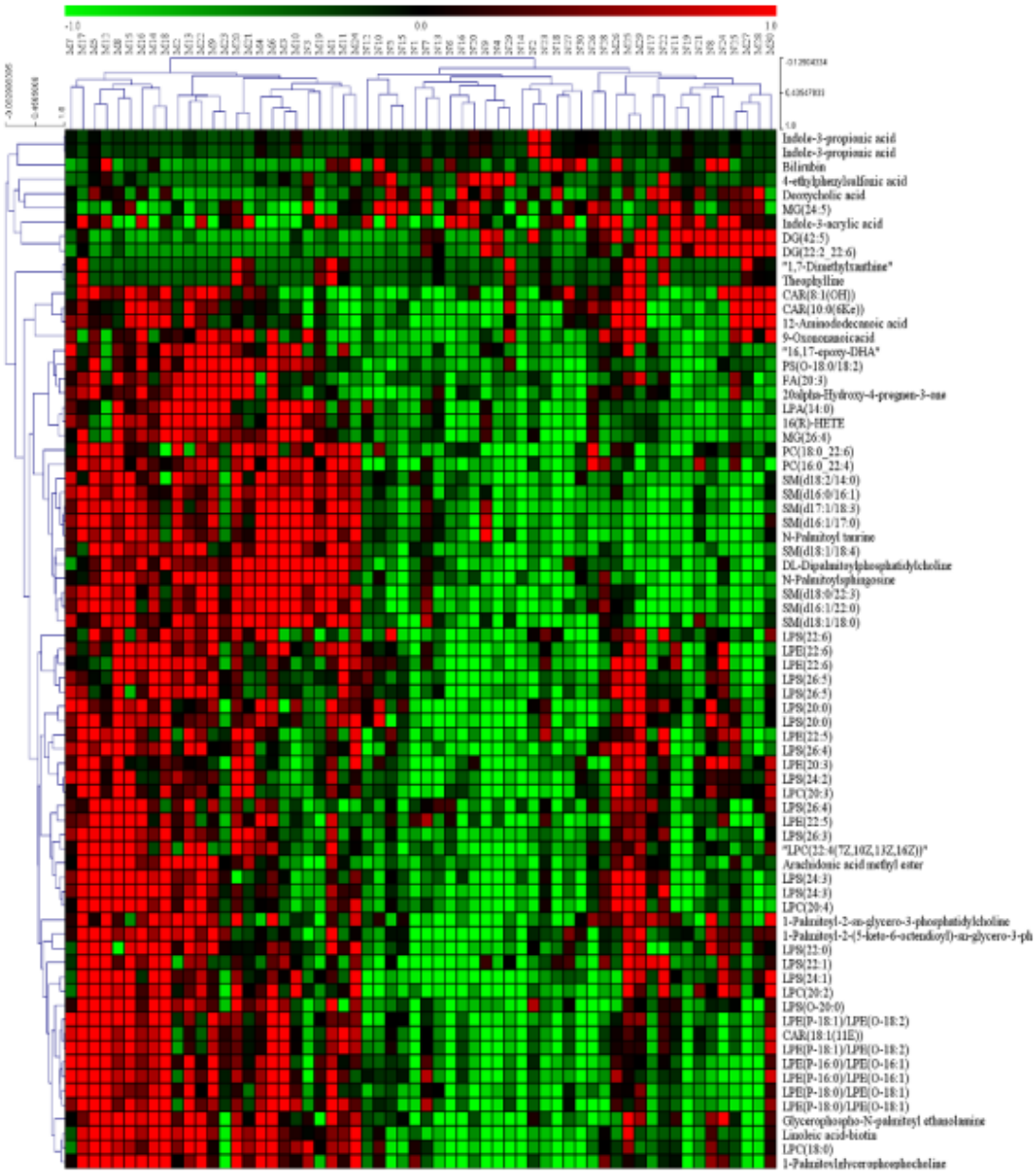

Figure 7

Heatmap visualization of differentially expressed metabolites in dyslipidemia. (N: Normal group; M: Model group; red means higher relative content, green means lower relative content).

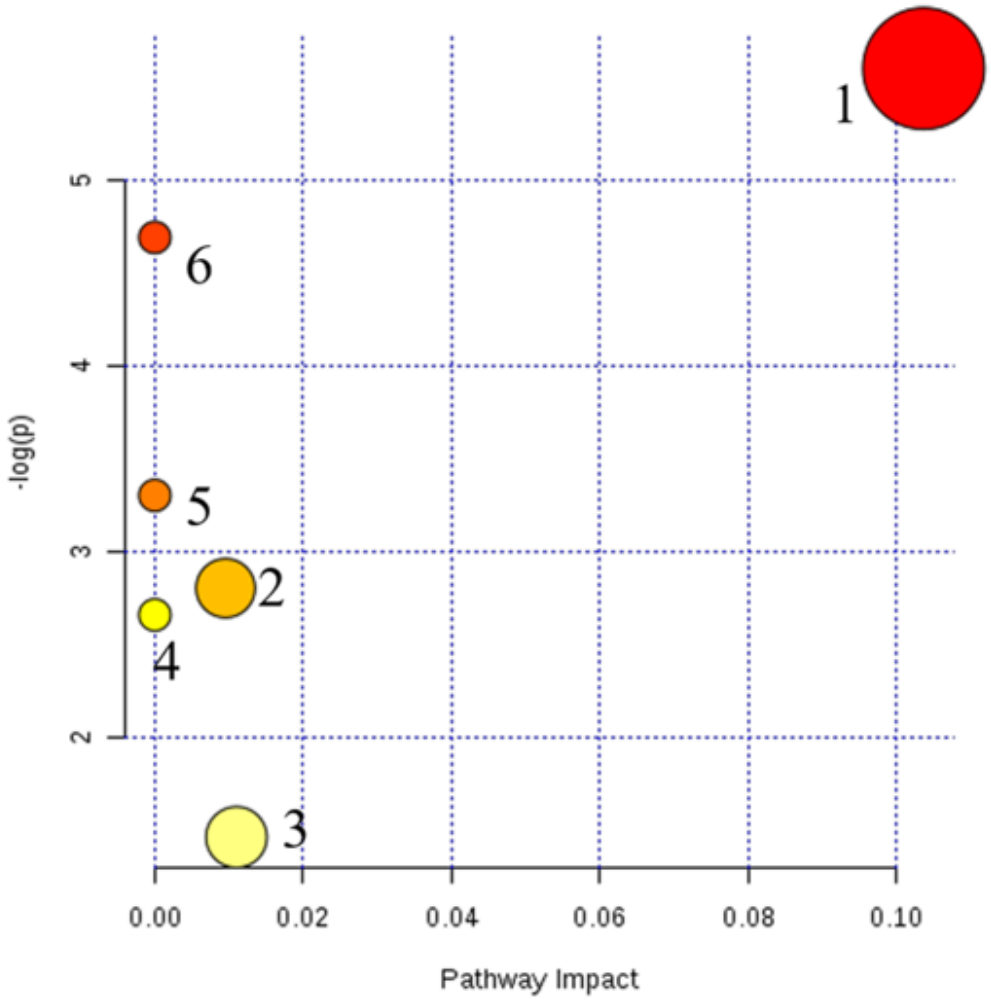

Figure 8

Overview of metabolic pathway analysis 1. Glycerophospholipid metabolism, 2. Sphingolipid metabolism, 3. Porphyrin metabolism, 4. Alpha-linolenic acid metabolism, 5. Linoleic acid metabolism, 6. Arachidonic acid metabolism